7. Plescia, J. B. & Saunders, R. S. *Proc. 11th Lunar planet. Sci. Conf.* 2423–2436 (1980).
8. Solomon, S. C. & Head, J. W. *Lunar planet. Sci.* **11**, 1063–1065 (1980).
9. Christensen, E. J. *J. geophys. Res.* **80**, 2909–2913 (1975).
10. *Topographic Map of Mars* (U.S. Geological Survey Miscellaneous Map I-961, 1976).
11. Downs, G. S., Mouginis-Mark, P. J., Zisk, S. H. & Thompson, T. W. *J. geophys. Res.* (in the press).
12. Downs, G. S., Mouginis-Mark, P. J., Zisk, S. H. & Thompson, T. W. *Lunar planet. Sci.* **13**, 182–183 (1982).
13. Thurber, C. H. & Toksöz, M. N. *Geophys. Res. Lett.* **5**, 977–980 (1978).
14. Schaber, G. G., Horstman, K. C. & Dial, A. L. *Proc. 9th Lunar planet. Sci. Conf.* 3433–3458 (1978).
15. Carr, M. H., Greeley, R., Blasius, K. R., Guest, J. E. & Murray, J. B. *J. geophys. Res.* **82**, 3985–4015 (1977).
16. Crumpler, L. S. & Aubele, J. C. *Icarus* **34**, 496–511 (1978).
17. Moore, H. J. & Hodges, C. A. *NASA-TM 82385* 266–268 (1980).
18. Downs, G. S., Reichley, P. E. & Green, R. R. *Icarus* **26**, 276–312 (1975).
19. Turcotte, D. L., Willemann, R. J., Haxby, W. F. & Norberry, J. *J. geophys. Res.* **86**, 3951–3959 (1981).
20. Comer, R. P., Solomon, S. C. & Head, J. W. *Lunar planet. Sci.* **11**, 171–173 (1980).
21. Scott, D. H. & Tanaka, K. L. *Icarus* **45**, 304–319 (1981).
22. Roth, L. E., Downs, G. S., Saunders, R. S. & Schubert, G. *Icarus* **42**, 287–316 (1980).
23. Macdonald, G. A. *Volcanoes* (Prentice-Hall, New Jersey, 1972).
24. Mouginis-Mark, P. J. *Proc. 12th Lunar planet. Sci. Conf.* 1431–1447 (1981).
25. Pike, R. J. & Clow, G. D. *Abstr. 3rd int. Colloq. Mars* 199–201 (Contr. 441, Lunar and Planetary Institute, Houston, 1981).
26. Walker, G. P. L. *Phil. Trans. R. Soc.* **A274**, 107–118 (1973).

A model of the Antarctic Ice Sheet

J. Oerlemans

Institute for Meteorology and Oceanography, University of Utrecht, Princetonplein 5, Utrecht 3508 TA, The Netherlands

Numerical modelling of ice sheets and glaciers has become a useful tool in glaciological research. A model described here deals with the vertical mean ice velocity, is time dependent, computes bedrock adjustment and uses an empirical diagnostic relationship to derive the distribution of ice thickness in ice shelves. The rate of snowfall and ice/snow melt depends on the (prescribed) sea-level temperature, surface slope, elevation and distance to open water. The model is able to reproduce the major features of the Antarctic Ice Sheet. When it is run to a steady state for present climatic conditions, the main difference with the present ice sheet is that the shallow parts of the Weddell Sea become covered by grounded ice.

TO understand ice-sheet histories from proxy data, and to see whether they are physically plausible, numerical ice-sheet models can have an important role. Although the theory of ice flow is formulated reasonably well (this does not apply to what happens at the ice–bedrock interface), modelling of large ice sheets requires a pragmatic approach. It is not possible to solve the full stress–strain rate relationships, together with the thermodynamic equation, for the whole Antarctic Ice Sheet, for example. This certainly applies if one wants to carry out integrations over 100,000 yr or so.

In recent years, ice-sheet models based on a flow law for the vertical mean ice velocity have become popular[1–4]; they have been used mainly for palaeoclimatic studies, and in complexity come between perfectly plastic models[5] and three-dimensional models[6]. In these models temperature is not calculated, so constant bulk flow parameters have to be used. In spite of the simplifications involved, the vertically integrated models capture most of the characteristics of large ice sheets.

Based on these observations, I have developed a vertically integrated model of the Antarctic Ice Sheet. In fact the Antarctic Ice Sheet is an excellent test case for the 'vertical mean approach', because it has a very irregular bedrock topography and subtle grounding line dynamics at some places, and its present-day physical characteristics are well documented[7].

The first version of the present model was used to investigate how sensitive the Antarctic Ice Sheet is to changes in the ice accumulation rate[2]. However, this version did not include bedrock adjustment and ice shelves, and could only be used for short integrations.

The second version, results of which are presented here, has much more internal freedom. The response of the bedrock topography to a varying ice load is computed, and a diagnostic relation for ice shelves (though simple) is included. A varying bedrock topography introduces the problem of initial conditions. It is not very well known how close the present bedrock topography is to isostatic equilibrium. A 100-m error in the equilibrium bedrock elevation will be insignificant in the central parts of the East Antarctic Ice Sheet, but is very important in such marginal regions as the Ross Sea.

Model description

The calculation of ice flow is based on a flow law relating vertical-mean horizontal ice velocity u to basal shear stress τ_b

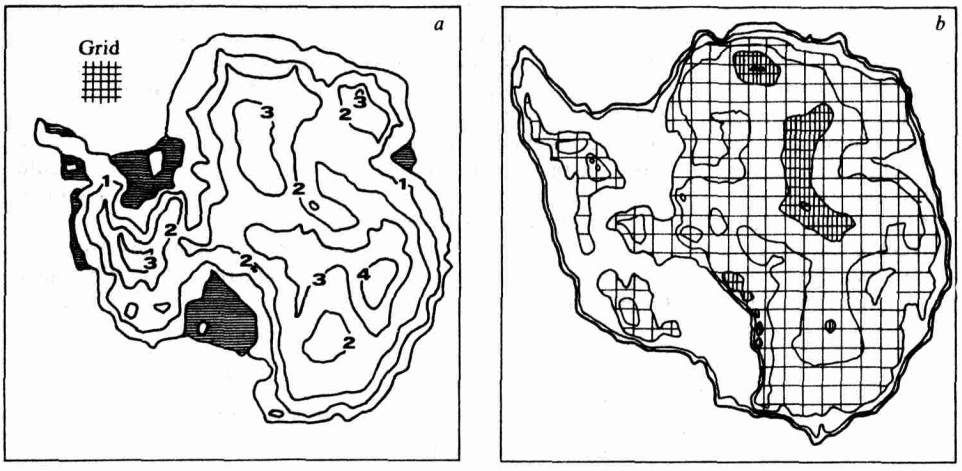

Fig. 1 *a*, Observed ice thickness as resolved on the model grid (part of which is shown in the upper left corner). Contour interval is 1 km. The major ice shelves are indicated by shading. *b*, Equilibrium bedrock topography in the case of no ice load. Contour interval is 1 km. The lowest contour level is 2 km below present sea level. Light shading indicates bedrock above sea level, heavy shading bedrock above the 2 km level. All input data are from ref. 10.

0028–0836/82/240550—04$01.00

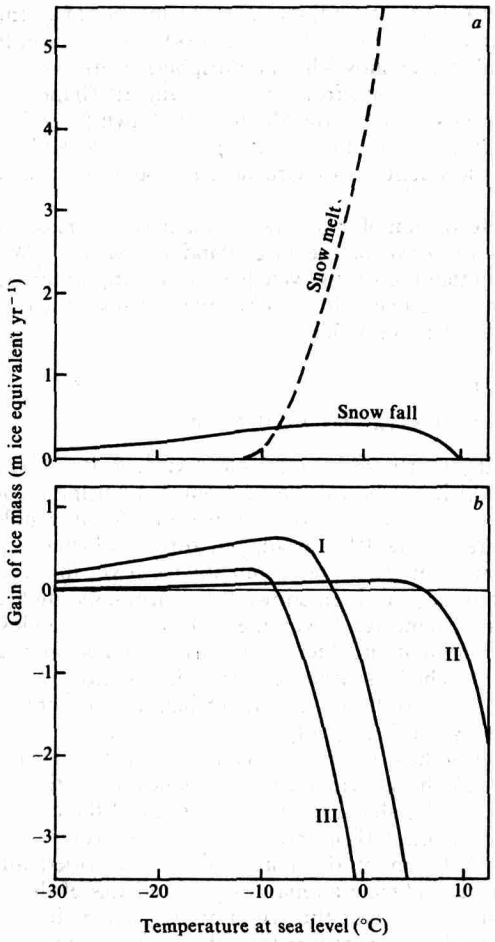

Fig. 2 Formulation of the mass balance, or ice accumulation rate, for the ice-sheet model. *a*, Dependence of snow/ice melt and snowfall on sea-level temperature for zero surface elevation and zero surface slope. *b*, The mass balance for different local conditions: I, a surface slope of 0.02 and elevation of 500 m, at the edge of the continent; II and III, the interior of the continent for elevations of 2,000 m and 0 m respectively.

(ref. 8). This law is of the Glen-type: $u = k\tau_b^m$, where k and m are flow parameters. The expression for u can be generalized to the two-dimensional case (involving assumptions that will not be discussed here), yielding the vertically integrated mass flow vector **M**:

$$\mathbf{M} = KH^{m+1}[\nabla H' \cdot \nabla H']^{(m-1)/2}\nabla H' \qquad (1)$$

where H is ice thickness, ∇ is the two-dimensional (horizontal) gradient operator and $H' = H + h$ is the surface elevation (h is the bedrock elevation with respect to sea level). So ice flows down the surface slope $\nabla H'$, and the rate at which this happens increases strongly with both ice thickness and surface slope. The evolution of the ice sheet is determined by the conservation of ice mass, that is

$$\partial H/\partial t = -\nabla \cdot \mathbf{M} + G \qquad (2)$$

G is the ice accumulation rate at the surface, expressed in units of ice depth per unit of time.

The response of the bedrock to the ice load is computed from:

$$\partial h/\partial t = -(h - h_0 + H/3.2)/T \qquad (3)$$

where h_0 is the equilibrium bedrock height without ice load. Equation (3) formulates a damped return, with time scale T, to local isostatic equilibrium. For loads with a horizontal length scale of more than a few hundred kilometres, equation (3) forms a good approximation[9]. For smaller loads, the flexural rigidity of the lithosphere becomes important. So, in general, equation (3) should work reasonably well, but for very small ice sheets or near the edge of a large ice sheet errors may occur (order of magnitude: 50 m).

Given the present bedrock topography and the distribution of ice thickness (Fig. 1*a*), and assuming that the present state of Antarctica is close to equilibrium, h_0 can be computed. Using data from the Russian Atlas of Antarctica[10], resolved on a grid with a spacing of 100 km, yields a no-ice bedrock topography h_0 as shown in Fig. 1b. This clearly shows how little of the bedrock beneath the present West Antarctic Ice Sheet is actually above sea level, even if the ice load is removed. Because we cannot be sure that the Antarctic Ice Sheet is close to a steady state, h_0 may be subject to errors. This applies in particular to the shallow Ross and Weddell seas, which were probably captured by grounded ice during the last ice age (20,000 yr ago). So it is possible that in these areas uplifting is still in progress[11]. Nevertheless, the bedrock topography displayed in Fig. 1*b* will serve as the initial condition for h, simply because a sound alternative is not available.

Ice shelves have to be taken into account to let the position of the grounding line be determined by the model. A prognostic equation for ice shelf growth/decay would not be feasible, because it would require a very small time step in the computations. Instead a diagnostic procedure is included. The thickness of floating ice at some point is calculated from the degree of enclosure (which is between 0° and 360°) by grounded ice, weighted with the distance to the grounding line and the ice thickness at the grounding line. In the present model only four directions (0°, 90°, 180° and 270°) are checked for each grid point to estimate the enclosure. An additional condition is that the ice shelf cannot be maintained if its thickness drops below 250 m. For an optimum choice of the proportionality constants appearing in this formulation, the calculated ice shelves for the

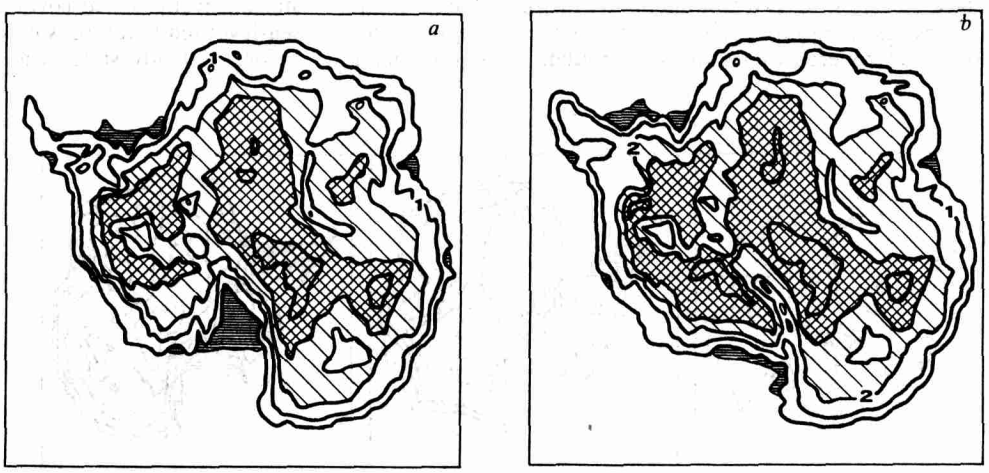

Fig. 3 Equilibrium states of the Antarctic Ice Sheet, computed with the numerical model for present sea level (*a*) and a sea-level stand of 100 m below the present one (*b*). In both integrations the initial condition was $H = 0$. Ice shelves are indicated by horizontal shading. Heavy lines are contours of ice thickness, except the outer one which gives the grounding line. The contour interval is 1 km. Light shading indicates ice thickness > 2 km, heavier shading ice thickness > 3 km.

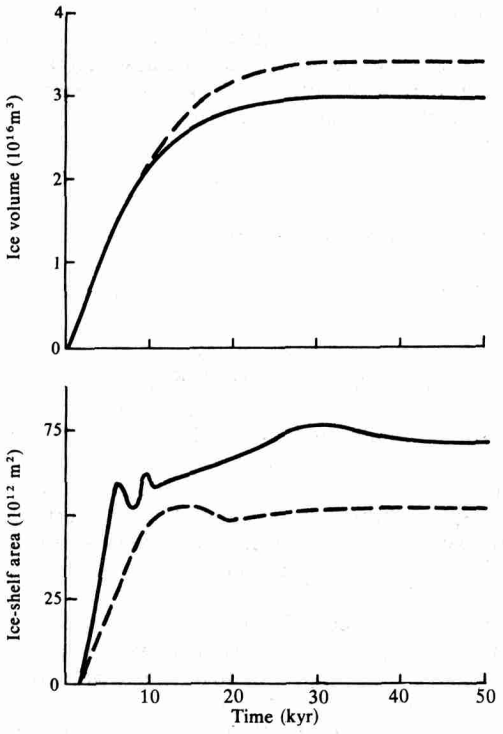

Fig. 4 Total ice volume and area covered by ice shelf, showing how the equilibrium states of Fig. 3 are reached. Solid line, experiment with present sea level; dashed line, experiment with the 100 m drop in sea level.

present distribution of grounded ice appear at the right locations with approximately the right thickness. Although ice-shelf dynamics does not explicitly occur in this procedure, it is dealt with in an implicit way, of course. It is no coincidence that ice shelves occur where the degree of enclosure is large. The compressive stresses associated with large enclosure counteract the ice thinning due to regular spreading. The present procedure mimics this mechanism well.

Because surface temperature and orographic enhancement of precipitation depend on the distribution of ice thickness, a general formulation for the ice accumulation rate G is desirable in which these effects appear in an explicit way. Based on the present distribution of surface elevation, surface slope and accumulation rate[10], the gain of ice mass due to precipitation is written as (in m ice equivalent yr^{-1}):

$$P = \max\left[0.05; f(\theta_0)(0.3 + 14\nabla H' - 4 * 10^{-5} H')/C\right] \quad (4)$$

So precipitation increases with surface slope and decreases with surface elevation. C is a 'continentality factor', which is computed by checking how many grid points in a circle of radius 500 km are covered by ice or bare ground. C ranges from 1 for an island of one grid point to 2 for the interior of a continent. The function $f(\theta_0)$, where θ_0 is sea-level temperature, models the dependence of snowfall on atmospheric water vapour content and the transition from snow to rain. Its shape is shown in Fig. 2*a*, in which a snowfall curve is drawn for $H' = 0$ and $\nabla H' = 0$. It is based on climatological practice and climatic change experiments with circulation models of the atmosphere[12,13].

Parameterization of ice/snow melt is based on mass-balance studies at the edge of the Greenland Ice Sheet[14]. With the assumption that the yearly cycle in surface temperature is more or less conserved in conditions of climatic change, the following approximate relation holds:

$$\begin{aligned} &\text{melt} = 0 && \text{if } \theta_s < -12\,^\circ\text{C} \\ &\text{melt} = (12 + \theta_s)^2 * 0.028 && \text{if } \theta_s \geq -12\,^\circ\text{C} \end{aligned} \quad (5)$$

as for P, the unit is m ice equivalent yr^{-1}; θ_s is surface temperature which can be calculated from θ_0 by using a constant lapse rate γ (so $\theta_s = \theta_0 + \gamma H'$). Equation (5) only holds for temperatures below 0 °C or so, but this is sufficient because higher temperatures do not permit any ice cover to survive.

The difference between snowfall and ice/snow melt makes up the mass balance G. Given the surface slope and elevation, and the continentality factor, it only depends on sea-level temperature. The first three factors are determined by the shape of the ice sheet itself. So climatic change experiments can be performed by varying θ_0 only.

To illustrate how the mass balance depends on local conditions, Fig. 2*b* shows $G(\theta_0)$ for three typical conditions: (I) on the edge of an ice sheet, (II) in the interior of the continent at 2,000 m elevation, (III) in the interior at sea level.

The formulation of the mass balance described above is capable of reproducing all major characteristics of the present mass-balance field over the Antarctic Ice Sheet. It adds considerably to the internal freedom of the model. For example, zones of high precipitation rate follow the edge of the ice sheet, which is certainly realistic.

All model equations are solved with a numerical scheme on a grid with 100-km spacing between the grid points (see Fig. 1*a*). The time step used is 10 yr. Model parameters not yet specified are: $m = 2.5$ and $K = 0.5$ m$^{-3/2}$ yr^{-1} (flow parameters), $T = 4{,}000$ yr (e-folding time scale for bedrock adjustment) and $\gamma = -8$°C km^{-1} (lapse rate). Values of K and m were found by tuning the model to the present Antarctic Ice Sheet for prescribed and fixed bedrock elevation, ice accumulation rate and grounding line. However, the choice is not crucial: other combinations of m and K can be found to give similar results.

Results

In the first experiment the model was run to a steady state starting from no ice cover and bedrock topography h_0. The sea-level temperature was set at −14 °C. It takes ~30,000 yr before a steady state is approached, so the integration was

Fig. 5 Equilibrium states of the model Antarctic Ice Sheet for θ_0, the annual sea-level temperature: *a*, $\theta_0 = 5$ °C; *b*, $\theta_0 = 0$ °C; *c*, $\theta_0 = -5$ °C. Heavy lines are contours of ice thickness (km). Ice shelves are indicated by horizontal shading.

carried out over 50,000 yr. This takes about 30 min central processor time on a CDC7600 computer.

The calculated ice distribution is shown in Fig. 3*a*. Comparing this with Fig. 1*a* shows that the model simulation is not too inaccurate, certainly not if one realizes that both bedrock elevations and mass balance are internally generated. Also, note that the state of Fig. 1*a* is not necessarily close to equilibrium, so that a sound judgement of the model performance cannot be made. The major difference between the simulated equilibrium state and the present observed state of the Antarctic Ice Sheet is the extension of grounded ice in the vicinity of the Antarctic Peninsula. In the model simulation a large part of the Weddell Sea is covered by grounded ice. As a consequence, the ice thickness in the western and central parts of the Antarctic Ice Sheet is larger, and the total ice volume is ~25% more than the presently observed volume.

The Ross Ice Shelf is well reproduced by the model, but the slope of the ice surface along the grounding line is steeper than observed. This is probably because the model does not take into account enhanced ice-mass discharge by extensive basal sliding (which is supposed to operate in these regions).

Figure 3*b* also shows the equilibrium state calculated for a sea-level stand which is 100 m below the present one. This was done to investigate the effect of glaciation in the Northern Hemisphere on the Antarctic ice volume. The experiment was identical to the first one (the same initial conditions) except for the 100-m sea-level drop.

Obviously, the West Antarctic Ice Sheet is sensitive to such a sea-level lowering: the grounding line in the Ross Sea advances hundreds of kilometres. At the upper (southern) tip of the Ross Sea, the ice thickness reaches 4 km. Grounding line advance in the Weddell Sea is less spectacular, because in the present-day simulation a large part of the shallow sea is already covered by grounded ice. Altogether, the volume of the West Antarctic Ice Sheet increases dramatically if the sea level lowers by 100 m. According to Fig. 4, the total ice volume increases by ~15%. If sea level is reset to its present value, the ice sheet appears to remain stable. Additional experiments revealed that a sea-level rise of at least 600 m is required to initiate grounding line instability in the Ross Sea (sea level temperature being equal). This suggests that in reality basal sliding must have had an important role in the deglacierization of the Ross Sea at the end of the last glacial extreme, because a 600 m sea-level rise did not occur, of course. Basal melting may have been present during the grounding-line advance, thus keeping the ice thickness of the 'Ross Ice Sheet' small, or it may be triggered by the Holocene climatic warming. However, such considerations are speculative.

So far sea-level temperature θ_0 has been kept constant. Note, however, how the model ice sheet reacts to changes in θ_0. Figure 5 shows steady-state ice sheets computed with $\theta_0 = 5, 0, -5$ °C respectively. For $\theta_0 = 5$ °C, the mass balance is positive only in mountainous regions. In general, the ice does not reach the coast but melts at the ice-sheet edge. For $\theta_0 = 0$ °C, the ice sheet covers most of the eastern part of the Antarctic continent, but ice cover in the western part is still restricted to higher regions. For $\theta_0 = -5$ °C, part of the West Antarctic Ice Sheet is formed, although the (present) Antarctic Peninsula is not yet attached to the main ice sheet. A further drop of θ_0 of a few °C creates the ice sheet shown in Fig. 3*a*. There is not much in between: a steady state in which the Weddell Sea is not covered by grounded ice did not appear.

An interesting feature in these experiments is the large ice thickness occurring for $\theta_0 = -5$ °C in the central parts of East Antarctica (compare with Fig. 3); this is due to the higher snowfall rates (see Fig. 2). However, such findings critically depend on the parameterization of the mass balance and should be considered with caution.

Discussion

The experiments described above should be considered as a first step in developing a more or less complete model of the Antarctic Ice Sheet. Fine tuning of the model has not yet been attempted and several physical processes are not yet included (for example, the impact of extensive basal sliding). So what can we learn from these experiments?

First, it seems that a vertically integrated model is capable of reproducing the influence of mountain ranges on the distribution of ice thickness. This is particularly clear if one considers an experiment in which the bedrock topography is fixed (see ref. 2). In that case the model simulation is very good and errors are only due to the poor resolution of some bedrock irregularities. In fact the value of the flow parameter K used in this study was found by tuning the fixed-bedrock model version to the present distribution of ice thickness. Even if the mass balance and bedrock elevation are free, the simulated ice sheet closely resembles the present Antarctic Ice Sheet. Moreover, because we do not know whether the ice cover in the Weddell Sea region represents an equilibrium state, we cannot state that the model result of Fig. 3 is in error (there is some evidence that ice cover on the Antarctic Peninsula is expanding[15]).

Experiments carried out by Budd and Smith[16] using a similar model of the Antarctic Ice Sheet produced results in agreement with those presented here, although they used a different flow law. This again demonstrates that for large-scale modelling of ice sheets the precise form of the flow law is not important: models can be easily tuned to give similar results.

The Quaternary history of the Antarctic Ice Sheet[17] seems to fit in the picture emerging from the numerical experiments. For a small sea-level drop (due to formation of ice sheets in the Northern Hemisphere) the ice sheet jumps to a state with large ice volume. It returns to a state with small ice volume only if sea level and sea-level temperature are sufficiently high (during a Northern Hemisphere interglacial). However, the required increase in sea level and/or temperature is very large and additional mechanisms are apparently needed to remove the grounded ice from the Ross and Weddell seas. Surging of the West Antarctic Ice Sheet could be one of them.

Future development of this model will include a more refined treatment of ice shelves, computation of the temperature field within the ice and a calculation of the effect of basal sliding on ice-mass discharge. In such a model ice surges may occur. Experiments with a one-dimensional model version including thermodynamics have shown that such events can be modelled very well by vertically integrated models[18]. The computational efficiency of the vertically integrated models (as compared with models with a grid in the vertical direction) will make it possible to study possible surging of the Antarctic Ice Sheet as a 'latitude–longitude problem' instead of looking along a steady flow line[19].

Received 8 February; accepted 20 April 1982.

1. Mahaffy, M. A. W. *J. geophys. Res.* **81,** 1059–1066 (1976).
2. Oerlemans, J. *J. Climatol.* **2,** 1–11 (1982).
3. Birchfield, G. E., Weertman, J. & Lunde, A. T. *Quat. Res.* (in the press).
4. Pollard, D. *Nature* **296,** 334–338 (1982).
5. Weertman, J. *Nature,* **261,** 17–20 (1976).
6. Jenssen, D. *J. Glaciol.* **18,** 373–390 (1977).
7. Budd, W. F., Jenssen, D. & Radok,,U. *Derived physical Characteristics of the Antarctic Ice Sheet* (Publ. No. 18 of Department of Meteorology, University of Melbourne, 1970).
8. Nye, J. F. *J. Glaciol.* **3,** 493–507 (1959).
9. Turcotte, D. L. *Adv. Geophys.* 51–86 (1979).
10. *Atlas Antarktiki* (Glawnoje Oeprawlenie geodezii i Kartografii MG, 1966).
11. Greischar, L. L. & Bentley, C. R. *Nature* **283,** 651–654 (1980).
12. Manabe, S. & Stouffer, R. J. *J. geophys. Res.* **85,** 5529–5554 (1980).
13. Oerlemans, J. & Vernekar, A. D. *Contr. atmos. Phys.* **54,** 352–361 (1981).
14. Ambach, W. *Polarforschung* **42,** 18–24 (1972).
15. Sugden, D. E. & Clapperton, C. M. *Nature* **286,** 378–381 (1980).
16. Budd, W. F. & Smith, I. N. *Annals Glaciol.* (in the press).
17. Thomas, R. H. & Bentley, C. R. *Quat. Res.* **10,** 150–170 (1978).
18. Oerlemans, J. *Free Oscillations of Polar Ice Sheets,* Preprint (University of Utrecht, 1982).
19. Budd, W. F. & McInnes, B. J. *Hydr. Sci. Bull.* **24,** 95–104 (1979).